Local electronic structure of intrinsic defects and impurities at the Fe(001) surface

Fang, C.M.; Groot, R.A. de; Bischoff, M.M.J.; Kempen, H. van

Published in:
Surface Science

DOI:
10.1016/S0039-6028(99)01057-2

Publication date:
2000

ELSEVIER

Surface Science 445 (2000) 123–129

surface science

www.elsevier.nl/locate/susc

Local electronic structure of intrinsic defects and impurities at the Fe(001) surface

C.M. Fang [a], R.A. de Groot [a,*], M.M.J. Bischoff [b], H. van Kempen [b]

[a] *Electronic Structure of Materials, Research Institute for Materials, Toernooiveld 1, 6525 ED Nijmegen, The Netherlands*
[b] *Experimental Solid State Physics 2, Research Institute for Materials, Toernooiveld 1, 6525 ED Nijmegen, The Netherlands*

Received 12 July 1999; accepted for publication 5 October 1999

Abstract

Ab-initio calculations for the electronic structure and magnetic properties of intrinsic defects and foreign impurities (oxygen and gold) on the Fe(001) surface using the LSW method and the super-cell approach are presented. The calculations show that the Fe intrinsic defects have different local density of states. The magnetic moment of the Fe substrate layer under the defects increases with decreasing number of nearest neighbors of the surface, while the magnetic moment of the Fe defects decreases with decreasing number of nearest neighbors on the surface. The oxygen impurities have rather narrow (2p) bands at about 6.0 eV below the Fermi energy. The influence of oxygen impurities on the Fe(001) surface states near the Fermi energy is remarkably insignificant. Both gold and oxygen impurities have small magnetic moments parallel to the surface iron.

Keywords: Density function calculations; Iron; Magnetic surfaces

1. Introduction

The high spatial resolution, both laterally and perpendicularly, of the scanning tunneling microscope (STM) to the surface created the possibility of real space imaging on the atomic scale [1–3]. However, it lacks a generally applicable method to discriminate between chemical elements [4,5]. Several methods have been developed to overcome this problem. Differences in work functions can be used in metals, as has been shown in the pioneering experiment of Binnig et al. [1–3]. Also, image states (which probe the work function in an indirect way) have been used for chemical identification [6]. The applicability of these techniques is limited by the rather small differences of the work functions for different metals and the fact that this parameter is strongly influenced by deviations of the surface from ideal low-index planes. In addition, the high bias voltage needed to observe the image states leads to a deterioration of the spatial resolution [6]. Another method suitable for metals, based on the theoretical works by Tersoff and Hamann [7–10], is the use of specific surface states, which have recently been observed with sharp features in the scanning tunneling spectroscopy (STS) of the bcc (001) surfaces of Fe and Cr [11].

The electronic structure of the iron(001) surface has been studied extensively not only because of the relatively simple ferromagnetic structure of the bulk iron, but also due to the availability of the near perfect, single-crystal, iron whisker substrates

* Corresponding author. Fax: +31-24-3652120.
E-mail address: robdg@baserv.uci.kun.nl (R.A. de Groot)

0039-6028/00/$ - see front matter
PII: S0039-6028(99)01057-2

[4,11–17]. Theoretical calculations showed the surface states to have not only a substantially enhanced magnetic moment, but also a sharp, very element-specific characteristic feature near the Fermi level, which has been used as the characteristic electronic fingerprints for the STS experiments [11,18,19]. However, the calculations by Nonas et al. showed that an iron adatom on the Fe(001) surface has a different magnetic moment and local electronic structure [20].

Gold is widely used to protect the iron surface from oxidation. Band structure calculations showed that the electronic structure and the magnetic moments of the interface iron are influenced by the existence of the covering gold layer [15]. On the Fe(001) surface, there are always possible intrinsic defects, as well as some foreign impurities, such as oxygen, or remaining gold. Oxygen contamination has been found in many cleaned surface systems [21,22]. Experiments showed that the oxidation process is already active at low exposures, and surface disorder could play a significant role [21–24]. There are theoretical calculations, but only for the Fe(001) surface covered by an ordered monolayer of oxygen [24,25]. Knowledge of the influence of the intrinsic defects and the impurities on the surface states is very important to understand the STS in order to obtain a chemical identification on the Fe(001) surface.

In this work, we present the results of ab-initio calculations for the electronic structure and magnetic moments of some intrinsic defects and extrinsic impurities (oxygen and gold) on the iron(001) surface using the localized spherical wave (LSW) method and the supercell approach. The relationship between the local magnetic moment and the coordination is investigated.

2. Calculations

Ab-initio band structure calculations were performed by the LSW method [26] using a scalar-relativistic Hamiltonian. We used local-spin-density (LSD) exchange-correlation potentials [27] inside space-filling and therefore overlapping spheres around the atomic constituents. The self-consistent calculations were carried out, including all core electrons. Iterations were performed with k-points distributed uniformly in an irreducible part of the first Brillouin zone (BZ), corresponding to a volume of the BZ per k-point of the order of 1×10^{-5}. Self-consistency was assumed when the changes in the local partial charges in each atomic sphere decreased to the order of 10^{-4}.

In the construction of the LSW basis [26,28,29], the spherical waves were augmented by solutions of the scalar-relativistic radial equations indicated by the atomic symbols 4s, 4p, 3d for Fe; 2s, 2p for O, and 6s, 6p, 5d for Au. The internal l summation used to augment a Hankel function at surrounding atoms was extended to $l=3$, resulting in the use of 4f orbitals for Fe, and 5f for Au. The vacuum between slabs is occupied by empty spheres, which employ functions 1s and 2p, and 3d as an extension. In this paper, we will discuss the charges on atoms. However, the charge on an atom cannot be defined in a unique way. Here, we will use the charge in the Wigner–Seitz spheres. The Wigner–Seitz radii of the Fe and Au atoms are the same as their corresponding bulk values. This ensures that the comparison of charges is meaningful.

The structure of the defects on the Fe(001) surface is built up on a supercell with the surface plane $a=b=2a_0$. The structures are schematically shown in Fig. 1. The calculations are performed for a series of intrinsic defects on the Fe(001) surface: (1) an adatom on Fe(001) surface is built by setting one adatom (Fe) on one of the four equal positions on the surface; (2) a structure of void is built by removing one Fe from the surface; (3) an iron step is simulated by doubling the cell in one direction perpendicular to the surface direction with only one of the iron positions occupied at surface for a slab of 13 layers of iron. The external defects are: (1) an oxygen adatom on the Fe(001) surface; (2) an oxygen in the Fe(001) surface replacing an iron atom; (3) a gold adatom on the Fe(001) surface; and (4) a gold step simulated by doubling the cell in one direction perpendicular to the surface direction only with one of the positions occupied by a gold atom at the surface. The oxygen–iron distance is set to be the O–Fe distance in FeO (2.15 Å), which comes from the experimental conclusions that in the initial

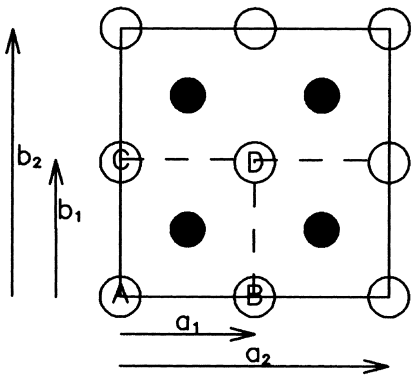

Fig. 1. Sketch of the structure of the Fe(001) surface covered by a submonolayer of defects (Fe, O, Au) in a $(2a \times 2a)$ supercell. The dashed circles represent the subsurface Fe atoms. The alphabets labeled on the atoms represents four structurally different positions. For a step on Fe(001), the positions A and C are occupied, while B and D are empty. For an adatom on the Fe(001) surface, only the position D is occupied. For a void on the Fe(001) surface, positions A, B and C are occupied, while D is unoccupied.

coverage, the oxygen always appears in the states of O^{-2} [21–24]. The Fe–Au distance is taken from the average of the distances in their bulk, as observed experimentally [30]. For all the systems, the inter-slab distances are larger than 10 Å, to avoid the interactions between slabs. This implies the introduction of eight monolayers of empty spheres with radii and positions equivalent to the iron atoms they replace as compared with the infinite solid. The charge in the central spheres of the vacuum was less than than 10^{-4} electrons.

3. Results and discussion

3.1. Electronic structure of intrinsic Fe defects

Table 1 lists the calculated results (electrons, magnetic moments and exchange splittings in the atomic spheres) for the intrinsic defects on the Fe(001) surface. Fig. 2 shows the local density of states for the intrinsic defects. The calculated local electronic structure for the Fe adatom is consistent with the results by Nonas et al. [20] using the local density theory and a KKR Green function method. Our calculated magnetic moment for the Fe adatom is 2.76 μ_B, in good agreement with the calculated data, 2.75 μ_B, in Ref. [20].

The surface Fe (adatom, step and atoms near the void) has very different shapes for the local density of states (Fig. 2), as well as the magnetic moments (Table 1). The 3d bands for the majority electrons are almost occupied for all kinds of Fe defects at the surface, as well as for the clean surface Fe case. The bandwidths of the Fe 3d states for majority electrons are similar. However, there is a greater density of 3d states for the majority electrons at the lower energy parts (about -4.0 eV), with increasing number of nearest neighbors at the surface (or the next-nearest neighbors in the iron bulk).

The characteristic Fe(001) surface states show a sharp peak near the Fermi energy for the minority electrons [11–15]. The local density of states for the minority electrons of the Fe adatom has an apparent crystal-field splitting (about 1.6 eV), with sharp peaks at about -0.2 and $+1.4$ eV, different from the surface states peaked at about -0.1 eV and about 1.0 eV for the clean Fe(001) surface (Fig. 2a and d). The local density of states for the Fe step and the Fe near the void shows no specific features near the Fermi energy (Fig. 2b and c). For the Fe step, the density of states of the minority electrons has an almost flat peak from about -1.2 eV to about the Fermi level, and a small peak at about 0.3 eV followed by a peak at about 1.0 eV. The Fe atom near the void also has a flat peak from -1.3 eV to -0.1 eV and two peaks at about $+0.2$ and $+1.2$ eV. The Fe atoms next nearest to the void have a sharp characteristic feature of surface states with a small shift up to about 0.2 eV above the Fermi energy, as shown in Fig. 2d.

The influence of coverage of the topmost layer on the iron substrate layer can be easily seen from Fig. 3: the local electronic structure of the substrate Fe layer becomes more bulk-like with increasing number of covering Fe atoms. While there are some states of the surface character at the energy range between the Fermi level and about 1.0 eV for the iron under an adatom (Fig. 3a), the local density of states of the substrate layer for the step and void systems, as well as the clean surface system, is already similar to the bulk, except for

Table 1
Interatomic distances of the nearest neighbors (NN) and next-nearest neighbors (NNN), the number of electrons, exchange splitting and the magnetic moments of the Fe atoms in the bulk and at the surfaces

	d_{Fe-Fe}(Å)	Q_{3d} (electrons)	ΔE_{3d}(eV)	M (μ_B)	Reference
Fe(bulk)	8×2.482 6×2.866	8.00	2.15	2.26	
Fe(110)	6×2.482 4×2.866			2.65	[31]
Fe(001)	4×2.482 5×2.866	7.50	2.66	2.91	
Fe(Void)	4×2.482 3×2.866	7.38	2.65	2.89	
Fe(Step)	4×2.482 3×2.866	7.46	2.60	2.85	
Fe(adatom)	4×2.482 1×2.866	7.36	2.53	2.76	
Fe(monolayer)	4×2.866	7.16	2.75	3.10	
Fe(atom)	0.0			4.0	

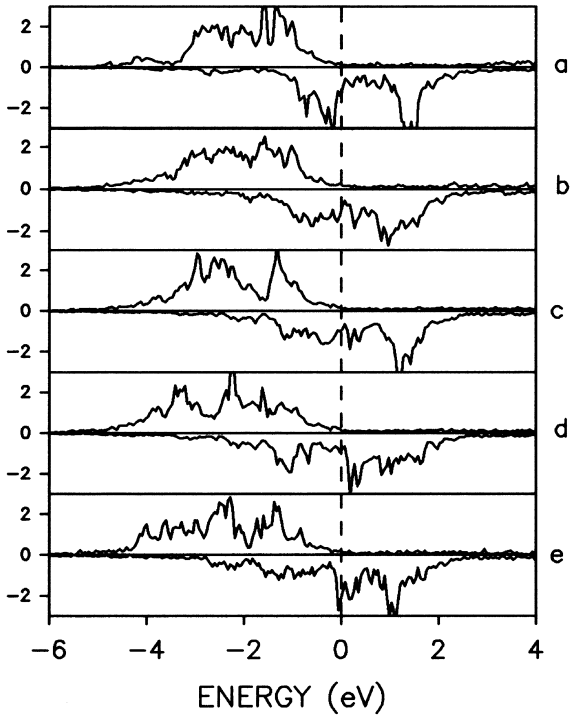

Fig. 2. Local density of states for the iron intrinsic defects at the Fe(001) surface: (a) Fe adatom; (b) Fe step; (c) Fe near a void; (d) Fe next near to a void, and (e) the clean Fe(001) surface. The Fermi energy is at zero (the same for the next figures).

some differences in detail for the structure and occupation of the minority states.

The magnetic moments, the number of valence electrons, and the number of nearest neighbors (NN) and next-nearest neighbors (NNN) of the substrate layer iron are listed in Table 2, because the number of next-nearest neighbors is the same for all the substrate Fe [note: here, the Fe(001) surface is regarded as a subsurface covered by a monolayer of empty spheres (Va)]. With the decreasing number of nearest neighbors (NN), the number of electrons decreases and the magnetic moment increases. The occupation of majority electron states is almost constant for all the substrate iron, which is consistent with the almost fully occupation of the 3d bands for the majority electrons, as shown in Fig. 3. The change in magnetic moment is due to combined effects of increasing occupation of the minority states and reduced exchange splitting. However, the iron atoms on the Fe(001) surface, which all have four nearest neighbors, show a different relationship between the magnetic moment and the coordination (Table 1): with the increasing number of nearest neighboring atoms on the Fe(001) surface [or the next-nearest neighbors (NNN) in the Fe bulk], the magnetic moment increases while the number of electrons increases. At the same time, the exchange splitting is almost constant.

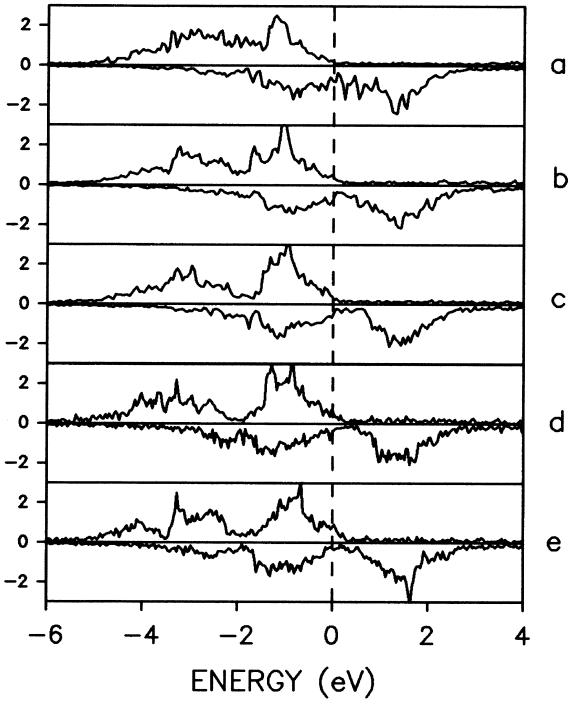

Fig. 3. Local density of states for the substrate Fe layer under the intrinsic defect: (a) adatom system; (b) step system; (c) void system; (d) the clean Fe(001) system, and (e) the bulk Fe.

The doubling of the unit cell in one direction perpendicular to the surface with only one iron position occupied leads to a structure with one type of iron at the substrate layer, two types of iron (one directly under the iron atom, the other under a vacuum position) at the subsurface, one type of iron at the next layer, etc. The behavior of the magnetic moments as a function of distance shows an oscillation. The outmost iron (step) has a magnetic moment of 2.85 μ_B, smaller than the clean Fe(001) (2.91 μ_B). The substrate iron has a magnetic moment of 2.57 μ_B, in between those of the clean (001) surface and its substrate. The behavior of the Fe atoms in the next layer shows a small screening effect: the iron under the step atom shows a more moderate reduction in magnetic moment (2.26 μ_B) than the iron atom under the unoccupied part of the surface (2.22 μ_B). The iron in the next layer is enhanced again (2.35 μ_B). The magnetic moment converges to its bulk value at the fourth layer. The screening effect is much weaker than that of the Fe(001) surface covered by gold [15].

3.2. Fe(001) surface with a submonolayer of foreign impurities

Fig. 4 shows the local density of states for the oxygen impurities and the Fe near the impurities. The O 2p bands for both atoms as an adatom and in the void at the Fe(001) surface are about 6.0 eV below the Fermi energy, which is in good agreement with the electron-energy loss spectroscopy (EELS) experiments by Sakasaka et al., who found the peak at 6.0 eV due to dissociative chemisorption of oxygen at the initial stage (oxygen concentration less than 3 L, $L=10^{-6}$ Torr) [20]. The O 2p bands have a width of about 0.7 eV (from -6.75 to -5.9 eV for the majority electrons, and from -6.1 eV to -5.5 eV for the minority electrons), which is narrower than the O 2p bands for the oxygen in the void (about 2.0 eV for both spin directions). The 2p bandwidths of the two kinds of impurities are narrower than that (about 4.0 eV) for an ordered monolayer coverage of oxygen on the Fe(001) surface [24,25]. The oxygen impurities also show an exchange splitting of about 0.1 eV.

Surprisingly, the local density of states for the substrate iron under the oxygen adatom, as well

Table 2
Magnetic moments and number of electrons of iron in the (001) substrate layer

	Fe/Fe(001)	Void/Fe(001)	Step/Fe(001)	Adatom/Fe(001)	Va/Fe(001)
Electrons	8.17	8.01	7.85	7.68	7.50
M (μ_B)	2.25	2.39	2.57	2.75	2.91
NN	8	7	6	5	4
NNN	5	5	5	5	5

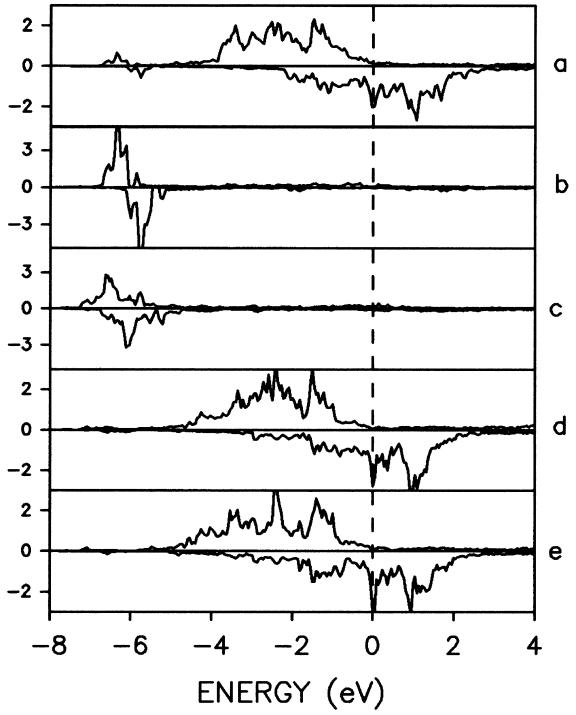

Fig. 4. Local density of states for the oxygen impurities at the Fe(001) systems: (a) the substrate Fe under the O adatom system; (b) an oxygen adatom on the Fe(001); (c) an oxygen in a void of the Fe(001) surface; (d) the iron near the O in the void; and (e) the iron next near to the O in the void.

as for the Fe atoms near the oxygen in voids, remains almost unchanged as compared to the clean Fe(001) surface (Fig. 4). For the iron atoms near the oxygen in the void, the local density of states shows a sharp characteristic feature of the surface states at about the Fermi energy, while the iron atom near an empty void shows no specific characteristic feature for the surface states (compare Figs. 2c and 4d).

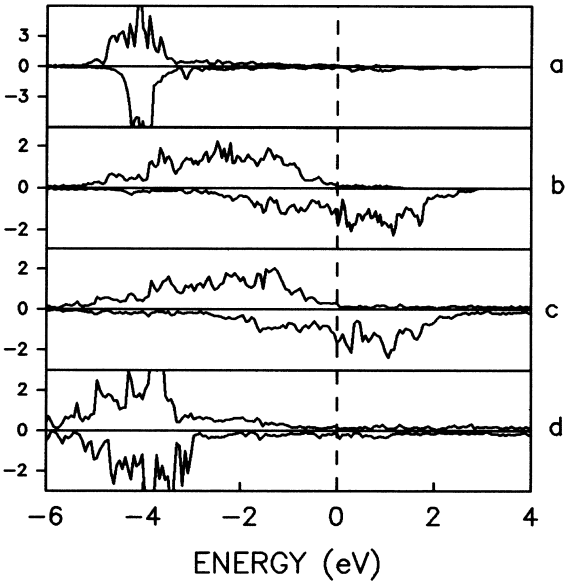

Fig. 5. Local density of states for the gold impurities at the Fe(001) surface: (a) an gold adatom on the Fe(001); (b) the substrate Fe under the gold adatom; (c) the substrate Fe under the gold step; and (d) the gold step.

As shown in Table 3, the oxygen impurities show small positive magnetic moments (0.16 μ_B for the O adatom, 0.11 μ_B for O in the void, respectively). The substrate iron under the oxygen adatom has a magnetic moment of 2.81 μ_B, smaller than the clean surface, while the iron near the oxygen in a void has a magnetic moment of 3.0 μ_B.

As shown in Fig. 5, the characteristic feature of the clean Fe(001) surface states almost disappears due to the gold impurities (the adatom or step). There is no apparent exchange splitting for the gold impurities. The gold impurities have a (5d) bandwidth of about 1.7 eV (from about −4.8 to

Table 3
Magnetic moments and number of electrons of the impurities and neighboring iron atoms at the Fe(001) surface

	O adatom		O in void[a]			Au adatom		Au step	
	O	$Fe_{sub.}$	O	Fe_{s1}	Fe_{s2}	Au	$Fe_{sub.}$	Au	$Fe_{sub.}$
Electrons	6.88	7.14	6.80	7.69	7.89	10.39	7.59	10.65	7.71
M (μ_B)	0.16	2.81	0.11	3.00	2.89	0.17	2.84	0.18	2.75

[a] Fe_{s1} is near to the oxygen, and Fe_{s2} the next near to the oxygen at the surface.

−3.5 eV) for the adatom, and about 2.5 eV (from −3.0 to −5.5 eV) for the step. The gold impurities show a small positive magnetic moment (about 0.18 μ_B), while the substrate layer has a magnetic moment of about 2.75 and 2.84 μ_B for the iron under the step and under the adatom, respectively.

4. Conclusions

Ab-initio band structure calculations have been performed for the intrinsic defects and impurities at the Fe(001) surface. The local densities of states of the cases considered (adatom, step, clean iron surface and iron atoms in the vicinity of a void) are different and could be used as a fingerprint in STM measurements. The size of the magnetic moment is mainly determined by the coordination. The magnetic moment increases with decreasing number of nearest iron neighbors. For cases where the number of nearest neighbors is constant, the magnetic moment decreases with decreasing number of next-nearest neighbors. The characteristic feature of the Fe(001) surface states has not been influenced significantly by oxygen impurities. However, the influence of gold impurities on the Fe(001) surface states is significant.

Acknowledgements

This work was part of the research program of the Stichting voor Fundamenteel Onderzoek der Materie (FOM) and was made possible by financial support from the Nederlandse Organisatie voor Wetenschappelijk Onderzoek (NWO).

References

[1] G. Binnig, H. Rohrer, Helv. Phys. Acta 55 (1982) 726.
[2] D. Binnig, H. Rohrer, C. Gerber, E. Weibel, Phys. Rev. Lett. 50 (1983) 120.
[3] G. Binnig, H. Rohrer, F. Salvan, Ch. Gerber, A. Baro, Surf. Sci. 157 (1985) L373.
[4] L.E.C. van de Leemput, H.vand Kempen, Rep. Prog. Phys. 55 (1992) 1165.
[5] F. Besenbacher, Rep. Prog. Phys. 59 (1996) 1737.
[6] T. Jung, Y.W. Mo, F.J. Himpsel, Phys. Rev. Lett. 74 (1995) 1641.
[7] J. Tersoff, D.R. Hamann, Phys. Rev. B 31 (1985) 805.
[8] R. Meservey, P.M. Tedrow, Phys. Rep. 238 (1994) 173.
[9] H. Dreysse, C. Demangeat, Surf. Sci. Rep. 28 (1997) 65.
[10] C.T. Campbell, Surf. Sci. Rep. 27 (1997) 1.
[11] J.A. Strocio, D.T. Pierce, A. Davies, R.J. Celotta, M. Weinert, Phys. Rev. Lett. 75 (1995) 2960.
[12] S. Ohnishi, A.J. Freeman, M. Weinert, Phys. Rev. B 28 (1983) 6741.
[13] M. Alden, S. Mirbt, H.L. Skiver, N.M. Rosengaard, B. Johansson, Phys. Rev B 46 (1992) 6303.
[14] S. Mirbt, O. Eriksson, B. Johansson, Phys. Rev B 52 (1995) 15070.
[15] C.M. Fang, R.A. de Groot, M.M.J. Bishop, H. van Kempen, Phys. Rev. B 58 (1998) 6772.
[16] A.M. Turner, J.L. Erskine, Phys. Rev. B 30 (1984) 6675.
[17] J. Tyson, A.H. Owens, J.C. Walker, J. Appl. Phys. 52 (1983) 2487.
[18] A. Biedermann, O. Genser, W. Heberstreit, M. Schmid, J. Redinger, R. Podloucky, P. Varga, Phys. Rev. Lett. 76 (1996) 4179.
[19] A. Davies, J.A. Stroscio, D.T. Pierce, R.J. Celotta, Phys. Rev. Lett. 76 (1996) 4175.
[20] B. Nonas, K. Wildberger, R. Zeller, P.H. Dederichs, J. Magn. Magn. Mater. 165 (1997) 137.
[21] M. Salvietti, P. Perro, R. Morono, M. Canepa, L. Mattera, Surf. Sci. 377–379 (1997) 481.
[22] R. Bertacco, M. Merano, F. Ciccacci, Appl. Phys. Lett. 72 (1998) 2050.
[23] Y. Sakisaka, T. Miyano, M. Onchi, Phys. Rev. B 30 (1984) 6849.
[24] A. Clarke, N.B. Brooks, P.D. Johnson, M. Weinert, B. Sinkovic, N.V. Smith, Phys. Rev. B 41 (1990) 9659.
[25] H. Huang, J. Hermanson, Phys. Rev. B 32 (1985) 6312.
[26] H. van Leuken, A. Lodder, M.T. Czyzyk, F. Springelkamp, R.A. de Groot, Phys. Rev. B 41 (1990) 5613.
[27] U. von Barth, B.I. Lundqvist, J. Phys. C 5 (1972) 1629.
[28] O.K. Anderson, O. Jepsen, Phys. Rev. Lett. 53 (1984) 2571.
[29] O.K. Anderson, Phys. Rev. B 8 (1975) 3060.
[30] Y.-L. He, G.-L. Wang, Phys. Rev. Lett. 71 (1993) 3834.
[31] R. Richter, J.G. Gay, J.R. Smith, Phys. Rev. Lett. 54 (1985) 2704.